Aberystwyth University

How robust are in-situ observations for validating satellite-derived albedo over the dark zone of the Greenland Ice Sheet?
Ryan, Jonathan; Hubbard, Alun; Irvine-Fynn, Tristram; Doyle, Samuel; Cook, J. M.; Stibal, Marek; Box, J. E.

How robust are in-situ observations for validating satellite-derived albedo over the dark zone of the Greenland Ice Sheet?

J. C. Ryan[1*], A. Hubbard[1,2], T. D. Irvine-Fynn[1], S. H. Doyle[1], J. M. Cook[3], M. Stibal[4] and J. E. Box[5]

[1]Centre for Glaciology, Institute of Geography and Earth Sciences, Aberystwyth University, Aberystwyth, UK

[2]Centre for Arctic Gas Hydrate, Environment and Climate, Department of Geology, University of Tromsø, Tromsø, Norway

[3]Department of Geography, University of Sheffield, Sheffield, UK

[4]Department of Ecology, Faculty of Science, Charles University, Vinicna 7, 128 44 Prague, Czech Republic

[5]Department of Glaciology and Climate, Geological Survey of Denmark and Greenland, Copenhagen, Denmark

*Corresponding author: Jonathan Ryan (jor44@aber.ac.uk)

Key Points:

- We test the validity of direct comparison between satellite-derived albedo and in-situ, AWS-based measurements over the Greenland Ice Sheet

- In-situ measurements across the ablation zone have too small a footprint to sample the full heterogeneity of surface ice as it melts

- Improved confidence in satellite measurements may be achieved by judicious selection of in-situ measurements for validation/calibration

Abstract

Calibration and validation of satellite-derived ice sheet albedo data require high-quality, in-situ measurements commonly acquired by up- and down-facing pyranometers mounted on automated weather stations (AWS). However, direct comparison between ground and satellite-derived albedo can only be justified when the measured surface is homogeneous at the length-scale of both satellite pixel and in-situ footprint. Here, we use digital imagery acquired by an unmanned aerial vehicle to evaluate point-to-pixel albedo comparisons across the western, ablating margin of the Greenland Ice Sheet. Our results reveal that in-situ measurements overestimate albedo by up to 0.10 at the end of the melt-season because the ground footprints of AWS-mounted pyranometers are insufficient to capture the spatial heterogeneity of the ice surface as it progressively ablates and darkens. Statistical analysis of 21 AWS across the entire Greenland Ice Sheet reveals that almost half suffer from this bias, including some AWS located within the wet snow zone.

1 Introduction

Surface albedo modulates the absorption of incoming shortwave radiation and is a primary factor governing the surface energy balance and ablation of the cryosphere [e.g., *Braithwaite and Olesen,* 1990; *Knap and Oerlemans,* 1996; *Brock et al.,* 2000; *van den Broeke et al.,* 2011]. Accurate measurements of albedo are therefore critical to understanding spatial patterns of melt, and an essential input to models for reliable prediction of surface runoff and the concomitant contribution of eustatic sea-level rise from glaciers and ice sheets. Due to its inherent spatial and temporal variability, interpolating surface albedo from extremely sparse in-situ measurements fails to represent albedo patterns realistically, particularly across the ablation zone. Hence, satellite remote-sensing provides the only practicable method for accurate determination of spatial and temporal patterns of snow and ice albedo for constraining regional climate, melt and runoff models across Greenland Ice Sheet and elsewhere [*Henderson-Sellers and Wilson,* 1983].

Retrieval of surface albedo from satellite data is a complex process, dependent on the performance of atmospheric correction and the accuracy of the angular model used to describe the bidirectional reflectance distribution function [BRDF; *Ricchiazzi et al.,* 1998; *Liang,* 2001; *Klein and Stroeve,* 2002; *Schaaf et al.,* 2002]. The calibration and validation of satellite albedo products therefore rely upon in-situ measurements, the majority of which are made by broadband pyranometers mounted on automated weather stations (AWS) [*Liang et al.,* 2005; *Stroeve et al.,* 2005, 2006, 2013]. However, direct comparison is only valid when the footprint of the in-situ measurement is either the same as the corresponding satellite image pixel or when the surface under scrutiny is homogeneous at the spatial scale of both the in-situ measurement and satellite data pixel [*Román et al.,* 2009, 2013; *Shuai et al.,* 2011].

To date, quality assessment and calibration of satellite-derived albedo across ice and snow make an implicit assumption of surface homogeneity [e.g., *Liang et al.,* 2005; *Stroeve et al.,* 2005, 2006, 2013], which may be valid across relatively flat and uniform snow surfaces, such as the accumulation zone of the Greenland and Antarctic Ice Sheets. However, below the transient snowline, particularly during the summer melt-season, ablating ice surfaces are not uniform. In Greenland, the ablation zone is comprised of a time-varying mixture of snow patches, ice with varying grain sizes, roughness features, biotic and abiotic impurities, and surface and shallow-subsurface water [*Bøggild et al.,* 2010; *Gardner and Sharp,* 2010; *Moustafa et al.,* 2015; *Ryan et al.*, 2017]. Ablating ice surfaces may therefore

not be homogeneous at the scale of both the in-situ measurement and the satellite pixel, leading to a potential discrepancy between the two measurements [*Knap and Oerlemans,* 1996]. Furthermore, because the in-situ measurement is assumed to be accurate, and indeed, is often considered a 'ground truth', discrepancies are frequently attributed to bias in the satellite-derived albedo product [e.g., *Stroeve et al.,* 2006]. This results in loss of confidence in satellite-derived albedo retrieval due to incorrect error attribution, thereby diminishing the statistical significance of long-term albedo trends and diluting capacity to accurately monitor the Earth's cryosphere [e.g., *Box et al.,* 2012; *He et al.*, 2013; *Stroeve et al.,* 2013; *Alexander et al.,* 2014].

This study investigates whether direct point-to-pixel comparisons for calibration and validation across the Kangerlussuaq (K-) transect of the Greenland Ice Sheet are justified. First, we evaluate the difference between in-situ albedo, measured at three AWS, and the MODerate resolution Imaging Spectroradiometer (MODIS) albedo product, MOD10A1. Second, we quantify the spatial heterogeneity of the satellite pixel, in which each AWS is situated, using 20 cm pixel resolution aerial imagery acquired by a fixed-wing unmanned aerial vehicle (UAV). Finally, we assess whether the spatial heterogeneity of the surface is captured by the AWS footprint and whether direct comparison with satellite-derived albedo data is robust and justified.
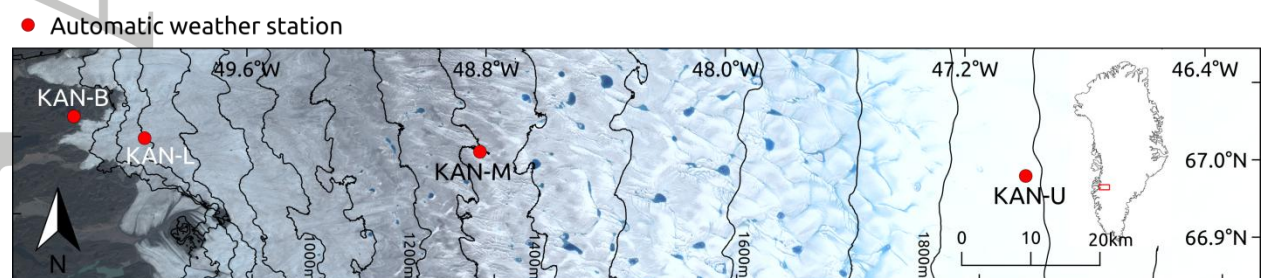
Figure 1. Locations of the K-transect AWS used in this study. The background is a Landsat 8 Operational Land Imager (OLI) true color image obtained on 9 July 2015.

2 Data and Methods

2.1 Satellite albedo

Satellite albedo retrievals between 2002 and 2016 were obtained from the MODIS daily albedo (300 to 3000 nm) product, MOD10A1 Collection 6 (C6), collected by NASA's Terra satellite [*Hall and Riggs,* 2016]. MOD10A1 is provided at 463 m (0.21 km²) pixel size, in a sinusoidal projection by the National Snow and Ice Data Center [NSIDC; *Hall and Riggs,* 2016]. MOD10A1 was chosen because it is commonly used for estimating spatial and temporal albedo trends across the Greenland Ice Sheet [e.g., *Box et al.,* 2012; *Alexander et al.,* 2014] and surface mass balance modeling [e.g., *van As et al.,* 2012]. Artefacts in MOD10A1 caused by undetected clouds, aircraft contrails or shadows were filtered using the 11-day statistics technique proposed by *Box et al.* [2012] (Text S1).

2.2 In-situ albedo

In-situ albedo measurements between 2009 and 2016 were obtained from three AWS (KAN-L, KAN-M and KAN-U) situated on the K-transect [Fig. 1, Text S2; *Ahlstrøm et al.,* 2008; *van As et al,* 2011]. Black thermopile Kipp & Zonen CNR1 or CNR4 net radiometers are mounted on the AWS, which measure downward and upward shortwave radiation fluxes with a specified uncertainty of less than 5% [*van den Broeke et al.,* 2004; *van As et al.,* 2012]. In the absence of accumulated snow, upward shortwave radiation is measured at a height of 2.8 m above the surface [*van As et al.,* 2011]. The instruments have a field of view (FOV) of 150° which yields a maximum ground footprint diameter of 21 m, equating to an area of 346 m². However, the effective footprint is smaller since the radiometers' cosine response means that they are inherently biased towards incident radiation at angles perpendicular to (i.e. from directly beneath) the sensor.

2.3 Quantifying surface spatial heterogeneity from aerial imagery

Visible wavelength (RGB) digital imagery was acquired by a fixed-wing UAV described by *Ryan et al.* [2015, 2017] (Text S3). We assume for the purposes of our analyses that the visible band imagery adequately captures the albedo variability of the surfaces surrounding the AWS. This assumption is justified since over half of the total solar energy arrives in the visible wavelengths [*Painter et al.,* 2012] and that most of the variability in reflected radiation for bare ice surfaces and snow with uniform grain size occurs in the visible band (350 to 695 nm) of the shortwave spectrum [*Warren and Wiscombe,* 1980*; Cutler and Munro*, 1996] where our Sony NEX-5N camera is most sensitive [*Jiang et al.,* 2013].

Semivariograms were constructed from the RGB aerial imagery to assess the spatial heterogeneity of the surfaces surrounding KAN-L and KAN-M (Text S4). The range of a semivariogram defines the distance from a point beyond which there is no further spatial correlation associated with that point [*Isaaks and Srivastava,* 1989; *Román et al.,* 2009, 2013]. We quantify this point by fitting an exponential function to the semivariogram and define the range (otherwise known as the practical sampling distance) as the ordinate value at which the exponential function reaches 99.9% of the maximum semivariance or sill. If the range is smaller than the AWS pyranometer footprint, then it is apparent that the in-situ measurement represents the spatial variability of the surface and can justifiably be used to validate MOD10A1. However, if the range is larger than the footprint of the in-situ measurement, then the AWS does not capture the full spatial variability of the surface, which would lead to a bias between AWS and MOD10A1 albedo.

| AWS	Annual		April/May		June		July	
	RMSD	Bias	RMSD	Bias	RMSD	Bias	RMSD	Bias
KAN-L	0.077	0.025	0.067	-0.029	0.073	0.072	0.100	0.100
KAN-M	0.038	0.013	0.028	-0.013	0.024	0.017	0.056	0.052
KAN-U	0.025	0.009	0.017	-0.009	0.022	0.013	0.026	0.017
Mean	**0.047**	**0.016**	**0.037**	**-0.017**	**0.040**	**0.034**	**0.061**	**0.056**

Table 1. RMSD and bias between albedo measured by the three K-transect AWS and MOD10A1 (2009 and 2016).

3 Results

## 3.1 Validation of satellite albedo using AWS

The mean annual RMSD between AWS and MOD10A1 albedo varies between 0.025 and 0.077 and has a mean of 0.047 (Table 1). The mean annual bias between AWS and MOD10A1 is positive for all three AWS on the K-transect (+0.016) suggesting that either MOD10A1 underestimates albedo or that the in-situ measurements overestimate albedo. The mean bias becomes more positive as the melt-season progresses from April/May (-0.017), to June (+0.034) and July (+0.056) and has a maximum of 0.10 at KAN-L (Table 1). The mean RMSD also increases from April/May (0.037) to June (0.040) and July (0.061) (Table 1). The MOD10A1-AWS bias has a statistically significant ($p < 0.001$) positive correlation with time since 1 April (Fig. 2a, b, c) and a statistically significant negative correlation with albedo (Fig. 2d, e, f).
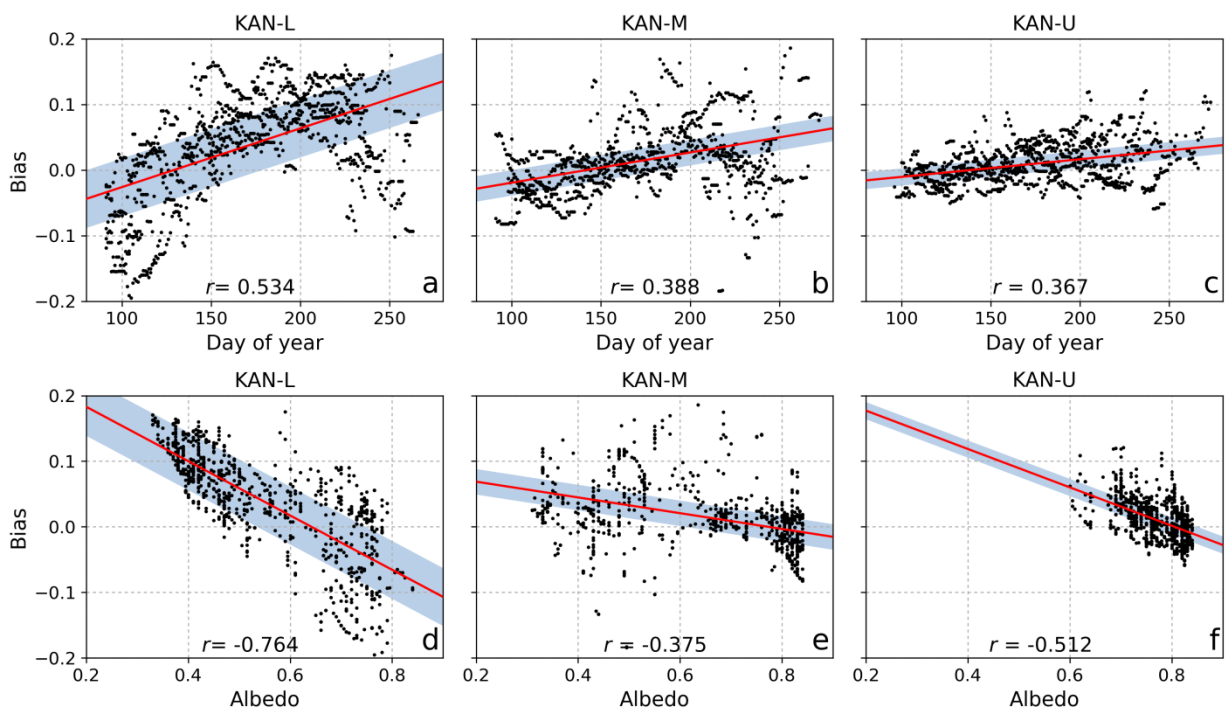
Figure 2. Relationship between MOD10A1-bias and (a, b, c) time since 1 April, and (d, e, f) albedo. The points represent every coincident observation from 2009 to 2016. All relationships are statistically significant to $p < 0.01$.

3.2 Spatial heterogeneity of ice sheet surface

Analysis of the UAV digital aerial imagery demonstrates that the surface of the ice sheet is spatially heterogeneous and changes significantly through time (Fig. 3). In June, the surface surrounding KAN-L is predominantly characterized by snow but it is not deep enough to obscure underlying changes in surface topography (Fig. 3a). By 14 July, the snow has completely melted leaving a predominantly bare ice surface with undulating topography (Fig. 3b). A relatively homogeneous snow surface characterizes KAN-M in June which is replaced by ponded meltwater and superimposed ice by July (Fig. 3c and d). The ice at the surface is characterized by different shades of grey, presumably depending on its saturation, crystallography and impurity load.
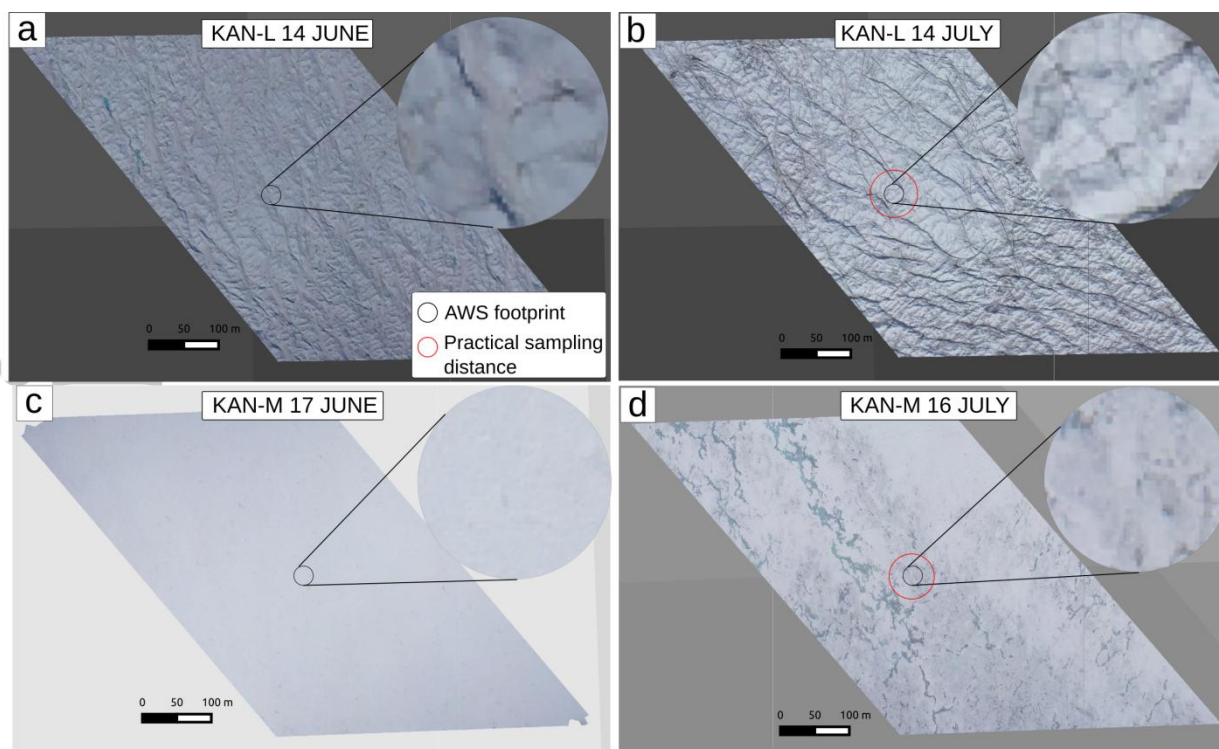
Figure 3. High resolution (20 cm) aerial images corresponding to the AWS locations within their respective MODIS pixels. The AWS footprint and practical sampling distance are shown by the black and red circles, respectively. The images are projected in UTM 22N.

Our derived semivariograms reveal that the practical sampling distance and area over which the inherent spatial variability of the ice sheet surface is captured, depends on both the time of year and the location (Fig. 4). In June, the exponential function attains the sill at separation distances of between 15 and 20 m indicating that albedo variability at these sites can be captured over relatively short sampling distances. Later in the melt-season, the semivariograms do not plateau until between 45 to 50 m revealing that longer sampling distances are necessary to capture the spatial variability of the ablating ice sheet albedo. Furthermore, the sill or maximum semivariance of the ice sheet surfaces increases by an order of magnitude at both KAN-L and KAN-M from June to July (Fig. 4). This indicates that the spatial heterogeneity of the ice sheet surface increases as the melt-season progresses.
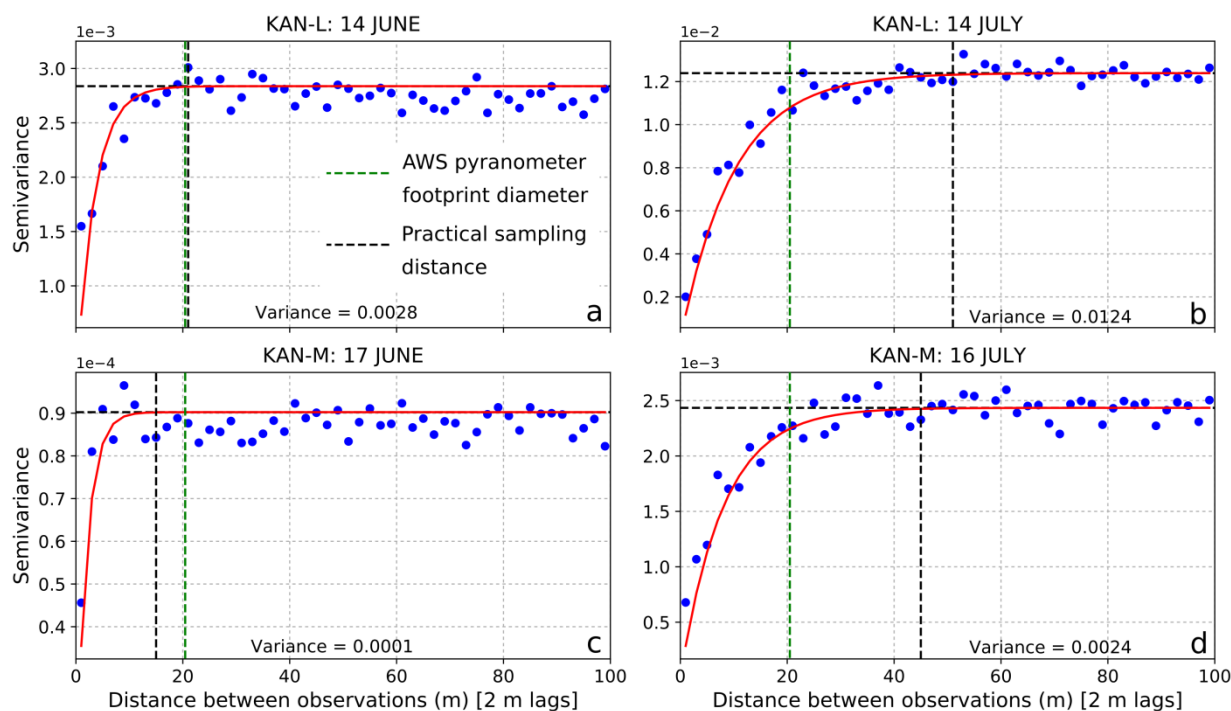
Figure 4. Semivariograms showing how the semivariance of the ice surface changes with increasing separation distance between samples between June and July. Between June and July, the sampling distance needed to capture the heterogeneity of the surface becomes larger than the 21 m diameter footprint of the AWS-mounted pyranometers. Note the varying y-axis scale.

4 Discussion and implications

Our analysis reveals that spatial variability in the melt processes and ablating surfaces across the Greenland Ice Sheet cause in-situ measurements on the K-transect to overestimate albedo (Table 1, Fig. 2). In June, our aerial imagery reveals that the, predominantly snow covered, surface is relatively homogeneous and that albedo sampled at length scales between 15 and 20 m is sufficient to capture that albedo variability (Fig. 3, 4). However, as the melt-season progresses, more bare ice is exposed, the albedo of the ablation zone reduces and sampling distances of between 45 and 50 m are required to fully represent the inherent heterogeneity of the ice surface and associated albedo reduction (Fig. 3, 4). The increase in surface heterogeneity is associated with an increase in the bias between AWS and MOD10A1 as represented by the negative correlation with albedo and positive correlation with time since 1 April (Table 1, Fig. 2). We therefore argue that the increase in the bias between MOD10A1 and AWS is a result of in-situ measurements becoming less representative of the surrounding surfaces [e.g. *Knap and Oerlemans,* 1996].

We argue that in-situ measurements mainly overestimate, rather than underestimate, albedo because the increase in spatial variability as the melt season progresses, is predominantly associated with an increase in the extent of low albedo surfaces (Fig. 3). These include bare ice with varying concentrations and types of impurity, cryoconite holes, surface water, crevasses and rough/steep topography, all of which have a lower albedo of between 0.10 and 0.27 [*Bøggild et al.,* 2010; *Ryan et al.,* 2016]. In-situ measurements are likely to undersample these darker surfaces because AWS are preferentially deployed on flat areas of

bare ice, rather than meltwater channels or crevasses, to reduce tilt and reduce the risk of loss or inundation. Such bare ice surfaces, with a mean albedo higher than 0.50 [*Ryan et al., 2016*], are inherently brighter than the albedo of the corresponding MOD10A1 pixel footprint, which will capture the larger area including lower albedo surface types. This results in a systematic discrepancy between the in-situ measurement and MOD10A1 product. Furthermore, as the melt-season progresses, the extent of impurity-rich bare ice, surface water and cryoconite holes tends to increase [e.g., *Fitzpatrick et al., 2014; Chandler et al., 2015*] which further drives this spatially-derived bias between in-situ and satellite albedo until snowfall resets the surface (Fig. 2).

The bias between MOD10A1 and KAN-U indicates that albedo overestimation is not limited to in-situ measurements in the ablation zone, but is also evident in the accumulation zone (Fig. 2e, f). Whilst KAN-U was out of range for our UAV imagery, given sustained sub-zero temperatures at an elevation of 1800 m a.s.l., we expect the surface to be snow covered, similar to KAN-M in mid-June (Fig. 3c). The point-to-pixel bias at KAN-U increases between April/May and July suggesting that the heterogeneity of the albedo over snow later in the melt-season is also insufficiently captured by the AWS pyranometer (Fig. 2e, f). An extended analysis of 21 Greenland AWS suggests that the bias due to spatial heterogeneity in surface types reported here for the K-sector of the ice sheet may potentially impact up to half of the PROMICE AWS network (Table S1, Fig. S1, S2). The bias between MOD10A1 and AWS has a significant ($p < 0.001$) negative correlation with albedo for nine (43%) AWS (Fig. S3, S4) and a significant positive correlation over time from 1 April for seven (33%) AWS (Fig. S5, S6).

Correlations are particularly strong for AWS in the ablation zone of the K-transect (Fig, S1, S2). These AWS are situated in the dark zone of the ice sheet where it has been reported that dust deposited in the accumulation zone throughout the Holocene is now emerging [*Wientjes et al., 2010; Shimada et al., 2016*]. The spatial variability and seasonal redistribution of this dust may cause the surface surrounding the K-transect AWS to be more heterogeneous than elsewhere on the ice sheet, leading to higher biases between MOD10A1 and AWS. At some sites outside of the K-transect, the AWS-MOD10A1 bias is negatively correlated over time from 1 April (Table S1, Fig. S5, S6). Surface processes may be responsible for these trends as well. For example, in the ablation zone, late-season snowfall which fills depressions and bridges gullies could preferentially increase the albedo of the surface outside of the AWS footprint [*Smeets and van den Broeke*, 2008]. Likewise, in the accumulation zone, the AWS may continue to observe the albedo of old snow during the melt-season because freshly fallen snow is redistributed away from the AWS but remains inside the corresponding MODIS pixel [*Lenaerts et al., 2014*]. We did not observe these processes in our UAV imagery and any testing of these specific hypotheses would require further UAV surveys over additional sites.

Improving the representativeness of in-situ albedo measurements can be achieved by increasing the height of the pyranometers above the surface (at 6.7 m the ground footprint would be 50 m), but this may be impractical for leveling the AWS and, even then, the cosine response of the pyranometers means that they would still be biased towards surfaces directly beneath them. Alternatively, attempts could be made to locate AWS at sites where the surface of the ice sheet is more homogeneous. These include areas of low strain where crevassing and fracturing is minimal, or where the distribution of impurities in the ice is more uniform. With this in mind, future research might benefit from installing local wireless networks of in-situ pyranometers within a single MODIS pixel for site-specific satellite validation exercises. We also recommend implementing UAV surveys and the techniques outlined in this study to characterize the spatial heterogeneity of the surface during visits to AWS. It is also worth

noting that other parameters measured by AWS used in regional climate and energy balance models may also suffer from the sampling biases documented here. For example, turbulent heat fluxes measured by AWS over flat surfaces are unlikely to truly represent complex flow over areas that have steep, rough and crevassed topography.

Confidence in MODIS albedo can be improved by systematically ignoring areas of the ice sheet with high spatial variability in validation exercises and only selecting representative in-situ measurements. Our analysis indicates that the most representative measurements are likely to be found in the dry snow zone or during April and May when the ice sheet surface consists of a more homogeneous snow surface. In both these cases, the assumption that the ice sheet surface is homogeneous at both the scale of in-situ and satellite image pixel is likely robust and the in-situ albedo provides a more justifiable validation of satellite albedo retrievals. However, we note that this would only verify the satellite albedo product for relatively simple, near-Lambertian scattering surfaces provided by snow, and would not hold true for the darker and optically complex ablating ice exposed later in the season.

It has previously been reported that Greenland Ice Sheet summer albedo declined by between 0.06 and 0.08 in the ablation zone and between 0.01 and 0.04 in the accumulation zone between 2000 and 2012 [*Box et al.,* 2012; *He et al.,* 2013; *Stroeve et al.,* 2013; *Alexander et al.,* 2014]. These long-term albedo trends are comparable to or below the 0.041 to 0.075 stated uncertainty of MODIS albedo products (e.g. MOD/MYD10A1 and MCD43A3) [e.g., *Stroeve et al.,* 2006, 2013; *Box et al.,* 2012] which raises questions regarding the true significance of these trends and current health of the cryosphere [e.g., *Polashenski et al.,* 2015]. However, these reported uncertainties are based on the assumption that in-situ AWS-based measurements provide an absolute ground-truth. Here, we show this assumption to be invalid for the ablating ice and snow over the K-transect. We argue that if unrepresentative in-situ measurements were removed from satellite validation exercises as outlined above, then the uncertainty in MODIS albedo products might be reduced to ~0.03. Such a result would improve statistical inferences regarding albedo decline across the Greenland Ice Sheet and, likewise at ablating ice masses elsewhere, increasing efficacy and confidence in the assimilation of albedo into regional climate and melt runoff models and prediction of global sea-level rise.

5 Conclusions

We investigated temporal patterns of bias between in-situ and satellite derived albedo at three AWS situated on the K-transect of the Greenland Ice Sheet. Aerial imagery acquired by a fixed-wing UAV allowed us to quantify the spatial heterogeneity at two AWS sites and determine whether comparison between albedo measured by in-situ measurements and satellite products is justified. Our results suggest that the ice sheet surface is not necessarily homogeneous at both the scale of the AWS pyranometer footprint and the MODIS pixel footprint and that caution must be exercised when validating satellite albedo retrievals using in-situ (e.g. AWS) measurements. At two sites in the ablation zone, aerial imagery demonstrates that AWS-mounted pyranometer footprints are insufficiently large to sample the true spatial heterogeneity of ice surface albedo in July, and hence the in-situ measurement cannot be justified as a valid ground truth. In-situ, AWS derived measurements tend to overestimate albedo, an issue that potentially affects almost half of the network of 21 AWS across the Greenland Ice Sheet that we analyzed and results in a degradation of precision and confidence in satellite-derived albedo products validated by this method.

Author contributions

JR and AH conceived the study and built the UAVs. JR carried out the the UAV surveys with assistance from JB. JR performed the MODIS-AWS comparisons and geostatistical analysis and wrote the manuscript. AH provided supervision. AH, JC and TI gave conceptual and technical advice and supported the interpretation of data. MS and JB organized, ran and funded the fieldwork and logistics, advised on the scope of the paper and commented on the text. All authors edited and critically revised the article.

Acknowledgments

References

Ahlstrøm, A. P., P. Gravesen, S. B. Andersen, D. van As, M. Citterio, R. S. Fausto, S. Nielsen, H. F. Jepsen, S. S. Kristensen, E. L. Christensen, L. Stenseng, R. Forsberg, S. Hanson, D. Petersen, and Team, P. P (2008), A new programme for monitoring the mass loss of the Greenland ice sheet, Geological Survey of Denmark and Greenland Bulletin, pp. 61–64.

Alexander, P. M., M. Tedesco, X. Fettweis, R. S. W. Van De Wal, C. J. P. P. Smeets, and M. R. Van Den Broeke (2014), Assessing spatio-temporal variability and trends in modelled and measured Greenland Ice Sheet albedo (2000-2013), The Cryosphere, 8, 2293–2312, doi:10.5194/tc-8-2293-2014.

Bøggild, C. E., R. E. Brandt, K. J. Brown, and S. G. Warren (2010), The ablation zone in northeast greenland: Ice types, albedos and impurities, Journal of Glaciology, 56, 101–113, doi:10.3189/002214310791190776.

Box, J. E., X. Fettweis, J. C. Stroeve, M. Tedesco, D. K. Hall, and K. Steffen (2012), Greenland ice sheet albedo feedback: thermodynamics and atmospheric drivers, The Cryosphere, 6, 821–839, doi:10.5194/tc-6-821-2012.

Braithwaite, R. J., and O. B. Olesen (1990), A simple energy-balance model to calculate ice ablation at the margin of the Greenland ice sheet, Journal of Glaciology, 36, 222-228, doi:10.3198/1990JoG36-123-222-228.

Brock, B. W., I. C. Willis, M. J., Sharp, and N. S. Arnold (2000), Modelling seasonal and spatial variations in the surface energy balance of Haut Glacier d'Arolla, Switzerland, Annals of Glaciology, 31, 53-62, doi:10.3189/172756400781820183.

Chandler, D. M., J. D. Alcock, J. L. Wadham, S. L. Mackie, and J. Telling (2015), Seasonal changes of ice surface characteristics and productivity in the ablation zone of the Greenland Ice Sheet, The Cryosphere, 9, 487–504, doi:10.5194/tc-9-487-2015.

Cutler, P. M., and D. S. Munro (1996). Visible and near-infrared reflectivity during the ablation period on Peyto Glacier, Alberta, Canada, Journal of Glaciology, 42, 333–340. doi: 10.1017/S0022143000004184.

Fitzpatrick, A. A. W., A. L. Hubbard, J. E. Box, D. J. Quincey, D. Van As, A. P. B. Mikkelsen, S. H. Doyle, C. F. Dow, B. Hasholt, and G. A. Jones (2014), A decade (2002-2012) of supraglacial lake volume estimates across Russell Glacier, West Greenland, The Cryosphere, 8, 107–121, doi:10.5194/tc-107-2014.

Gardner, A. S., and M. J. Sharp (2010), A review of snow and ice albedo and the development of a new physically based broadband albedo parameterization, Journal of Geophysical Research, 115, F01009, doi:10.1029/2009JF001444.

Hall, D. K., and G. A. Riggs, (2016) MODIS/Terra Snow Cover Daily L3 Global 500m Grid, Version 6, NASA National Snow and Ice Data Center Distributed Active Archive Center, Boulder, Colorado USA, doi:10.5067/MODIS/MOD10A1.006.

He, T., S. Liang, Y. Yu, D. Wang, F. Gao, and Q. Liu (2013), Greenland surface albedo changes in July 1981–2012 from satellite observations. Environmental Research Letters, 8(4), p.044043, doi:10.1088/1748-9326/8/4/044043.

Henderson-Sellers, A., and M. F. Wilson (1983), Surface albedo data for climate modeling, Reviews of Geophysics, 21, 1743–1778, doi:10.1029/RG021i008p01743.

Isaaks, E. H. and R. M. Srivastava (1989), Applied geostatistics, Oxford University Press, New York, USA.

Jiang, J., D. Liu, J. Gu, and S. Susstrunk (2013), What is the space of spectral sensitivity functions for digital color cameras?, Proceedings of IEEE Workshop on Applications of Computer Vision, pp. 168–179, doi:10.1109/WACV.2013.6475015.

Klein, A. G., and J. Stroeve (2002), Development and validation of a snow albedo algorithm for the MODIS instrument, Annals of Glaciology, 34(1), 45–52, doi:10.3189/172756402781817662.

Knap, W. H., and J. Oerlemans (1996) The surface albedo of the Greenland ice sheet: satellite-derived and in situ measurements in the Søndre Strømfjord area during the 1991 melt season. Journal of Glaciology, 42(141), doi:10.3198/1996JoG42-141-364-374.

Lenaerts, J. T. M., M. R. van den Broeke, J. H. van Angelen, E. van Meijgaard, and S.J. Déry (2012), Drifting snow climate of the Greenland ice sheet: a study with a regional climate model, The Cryosphere, 6, 891-899, doi:10.5194/tc-6-891-2012, 2012.

Liang, S (2001), Narrowband to broadband conversions of land surface albedo I: Algorithms, Remote Sensing of Environment, 76(2), 213–238, doi:10.1016/S0034-4257(00)00205-4.

Liang, S., J. Stroeve, and J. E. Box (2005), Mapping daily snow/ice shortwave broadband albedo from Moderate Resolution Imaging Spectroradiometer (MODIS): The improved direct retrieval algorithm and validation with Greenland in situ measurement, Journal of Geophysical Research D: Atmospheres, 110, 1–10, doi:10.1029/2004JD005493.

Moustafa, S. E., A. K. Rennermalm, L. C. Smith, M. A. Miller, J. R. Mioduszewski, L. S. Koenig, M. G. Hom and C. A. Shuman (2015), Multi-modal albedo distributions in the ablation area of the southwestern Greenland Ice Sheet, The Cryosphere, 9, 1–11, doi:10.5194/tc-9-1-2015.

Painter, T.H., S. M. Skiles, J. S. Deems, A. C. Bryant, C. C. Landry (2012), Dust radiative forcing in snow of the Upper Colorado River Basin: 1. A 6 year record of energy balance, radiation, and dust concentrations. Water Resources Research, 48(7), doi:10.1029/2012WR011985.

Polashenski, C. M., J. E. Dibb, M. G. Flanner, J. Y. Chen, Z. R. Courville, A. M. Lai, J. J. Schauer, M. M. Shafer, and M. Bergin (2015), Neither dust nor black carbon causing apparent albedo decline in Greenland's dry snow zone; implications for MODIS C5 surface reflectance, Geophysical Research Letters, 42, 9319–9327, doi:10.1002/2015GL065912.

Ricchiazzi, P., S. Yang, C. Gautier, and D. Sowle (1998), SBDART: A research and teaching software tool for plane-parallel radiative transfer in the Earth's atmosphere, Bulletin of the American Meteorological Society, 79(10), 2101-2114, doi:10.1175/1520-0477(1998)079<2101:SARATS>2.0.CO;2.

Román, M. O., C. B. Schaaf, C.E. Woodcock, A. H. Strahler, X. Yang, R. H. Braswell, P. S. Curtis, K. J. Davis, D. Dragoni, M. L. Goulden, L. Gu, D. Y. Hollinger, T. E. Kolb, T. P. Meyers, J. W. Munger, J. L. Privette, A. D. Richardson, T. B. Wilson and S. C. Wofsy (2009), The MODIS (Collection V005) BRDF/albedo product: Assessment of spatial representativeness over forested landscapes, Remote Sensing of Environment, 113(11), 2476–2498, doi:10.1016/j.rse.2009.07.009.

Román, M. O., C. K. Gatebe, Y. Shuai, Z. Wang, F. Gao, J. G. Masek, T. He, S. Liang and C. B. Schaaf (2013), Use of in situ and airborne multiangle data to assess MODIS-and Landsat-based estimates of directional reflectance and albedo, IEEE Transactions on Geoscience and Remote Sensing, 51, 1393–1404, doi:10.1109/TGRS.2013.2243457.

Ryan, J. C., A. L. Hubbard, J. E. Box, J. Todd, P. Christoffersen, J. R. Carr, T. O. Holt and N. Snooke (2015), UAV photogrammetry and structure from motion to assess calving dynamics at Store Glacier, a large outlet draining the Greenland ice sheet, The Cryosphere, 9, 1–11, doi:10.5194/tc-9-2015.

Ryan, J. C., A. Hubbard, M. Stibal, J. E. Box and team, T. D. S. P (2016), Attribution of Greenland's ablating ice surfaces on ice sheet albedo using unmanned aerial systems, The Cryosphere Discussions, 2016, 1–23, doi:10.5194/tc-2016-204.

Ryan J. C., A. Hubbard, J. E. Box, S. Brough, K. Cameron, J. M. Cook, M. Cooper, S. H. Doyle, A. Edwards, T. Holt, T. Irvine-Fynn, C. Jones, L. H. Pitcher, A. K. Rennermalm, L. C. Smith, M. Stibal and N. Snooke (2017), Derivation of high spatial resolution albedo from UAV digital imagery: Application over the Greenland Ice Sheet. Front. Earth Sci. 5:40. doi: 10.3389/feart.2017.00040

Schaaf, C. B., F. Gao, A. H. Strahler, W. Lucht, X. Li, T. Tsang, N. C. Strugnell, X. Zhang, Y. Jin, J. P. Muller, P. Lewis, M. Barnsley, P. Hobson, M. Disney, G. Roberts, M. Dunderdale, C. Doll, R. P. d'Entremont, B. Hu, S. Liang, J. L. Privette and D. Roy (2002), First operational BRDF, albedo nadir reflectance products from MODIS, Remote sensing of Environment, 83, 135–148, doi:10.1016/S0034-4257(02)00091-3.

Shimada, R., N. Takeuchi, and T. Aoki (2016), Inter-annual and geographical variations in the extent of bare ice and dark ice on the Greenland Ice Sheet derived from MODIS satellite images, Frontiers in Earth Science, 4, doi: 10.3389/feart.2016.00043.

Shuai, Y., J. G. Masek, F. Gao and C. B. Schaaf (2011) An algorithm for the retrieval of 30-m snow-free albedo from Landsat surface reflectance and MODIS BRDF, Remote Sensing of Environment, 115(9), 2204–2216, doi:10.1016/j.rse.2011.04.019.

Smeets, C. J. P. P. and M. R. van den Broeke (2008), Temporal and spatial variations of the aerodynamic roughness length in the ablation zone of the Greenland Ice Sheet, Boundary-Layer Meteorology, 128, doi:10.1007/s10546-008-9291-0.

Steffen, K., and J. E. Box (2001), Surface climatology of the Greenland ice sheet: Greenland Climate Network 1995 - 1999, Journal of Geophysical Research, 106, 951–964, doi:10.1029/2001JD900161.

Stroeve, J. C., J. E. Box, F. Gao, S. Liang, A. Nolin, and C. Schaaf (2005), Accuracy assessment of the MODIS 16-day albedo product for snow: comparisons with Greenland in situ measurements, Remote Sensing of Environment, 94, 46–60, doi:10.1016/j.rse.2004.09.001.

Stroeve, J. C., J. E. Box, and T. Haran (2006), Evaluation of the MODIS (MOD10A1) daily snow albedo product over the Greenland ice sheet, Remote Sensing of Environment, 105, 155–171, doi:10.1016/j.rse.2006.06.009.

Stroeve, J. C., J. E. Box, Z. Wang, C. Schaaf, and A. Barrett (2013), Re-evaluation of MODIS MCD43 Greenland albedo accuracy and trends, Remote Sensing of Environment, 138, 199–214, doi:10.1016/j.rse.2013.07.023.

van As, D (2011),Warming, glacier melt and surface energy budget from weather station in the Melville Bay Greenland, Journal of Glaciology, 57(202), 208–220, doi:10.3189/002214311796405898.

van As, D., A. L. Hubbard, B. Hasholt, A. B. Mikkelsen, M. R. van den Broeke, and R. S. Fausto (2012), Large surface meltwater discharge from the Kangerlussuaq sector of the Greenland ice sheet during the record-warm year 2010 explained by detailed energy balance observations, The Cryosphere, 6, 199–209, doi:10.5194/tc-6-199-2012.

van den Broeke, M., D. van As, C. Reijmer, and R. S. W. van de Wal (2004), Assessing and improving the quality of unattended radiation observations in Antarctica, Journal of Atmospheric and Oceanic Technology, 21, 1417–1431, doi:10.1175/1520-0426(2004)021<1417:AAITQO>2.0.CO;2.

van den Broeke, M. R., C. J. P. P. Smeets, and R. S. W. van de Wal (2011), The seasonal cycle and interannual variability of surface energy balance and melt in the ablation zone of the west Greenland ice sheet, The Cryosphere, 5, 377-390, doi:10.5194/tc-5-377-2011.

Warren, S. G., W. J. Wiscombe (1980), A model for the spectral albedo of snow. II: Snow containing atmospheric aerosols, Journal of Atmospheric Science, 37, 2734-2745, doi: 10.1175/1520-0469(1980)037<2734:AMFTSA>2.0.CO;2.

Wientjes, I. G. M., and J. Oerlemans (2010), An explanation for the dark region in the western melt zone of the Greenland ice sheet. The Cryosphere, 4, 261–268, doi: 10.5194/tc-4-261-2010.